

Tectonic plate under a localized boundary stress: fitting of a zero-range solvable model

This article has been downloaded from IOPscience. Please scroll down to see the full text article.

2008 J. Phys. A: Math. Theor. 41 085206

(<http://iopscience.iop.org/1751-8121/41/8/085206>)

View [the table of contents for this issue](#), or go to the [journal homepage](#) for more

Download details:

IP Address: 171.66.16.153

The article was downloaded on 03/06/2010 at 07:29

Please note that [terms and conditions apply](#).

Tectonic plate under a localized boundary stress: fitting of a zero-range solvable model

L Petrova¹ and B Pavlov^{1,2}

¹ VA Fock Institute of Physics, St Petersburg University, Russia

² Department of Mathematics, the University of Auckland, New Zealand

Received 1 June 2007, in final form 5 December 2007

Published 12 February 2008

Online at stacks.iop.org/JPhysA/41/085206

Abstract

We suggest a method of fitting of a zero-range model of a tectonic plate under a boundary stress on the basis of comparison of the theoretical formulae for the corresponding eigenfunctions/eigenvalues with the results extraction under monitoring, in the remote zone, of non-random (regular) oscillations of the Earth with periods 0.2–6 h, on the background seismic process, in case of low seismic activity. Observations of changes of the characteristics of the oscillations (frequency, amplitude and polarization) in course of time, together with the theoretical analysis of the fitted model, would enable us to localize the stressed zone on the boundary of the plate and estimate the risk of a powerful earthquake at the zone.

PACS numbers: 01.45.D, 02.30.Jr, 02.30.Tb

1. Dynamics of the system of tectonic plates and the motivation of the zero-range model

The lithosphere of Earth consists of 14 tectonic plates which jigsaw fit each other. The plates are isolated from underlying solid structures within the Earth mantle by the low-viscosity layer of the asthenosphere which is formed, due to various conditions, including high pressure and temperature, in the interval of depth 100–200 km. The plates move on the surface of Earth, due to convective flows and variations of the angular speed of Earth, gliding on the low-viscosity layer of asthenosphere and interacting with each other at some *active boundary zones*, see below. Figure 1 shows a complex form of boundaries between tectonic plates and their movements in different directions³. The plates are enumerated in the following order: 1. South-American plate, 2. African plate, 3. Somali plate, 4. Indian and Australian plates, 5. Pacific plate, 6. Nazca plate, 7. North-American plate, 8. Philippines plate, 9. Euro-Asian plate, 10. Antarctic plate, 11. Caribbean plate, 12. Cocos plate, 13. Arabian plate.

³ Figure 1 is borrowed from the book of Aplonov [3], and is included in our text with permission of the publishing house of the St Petersburg University.

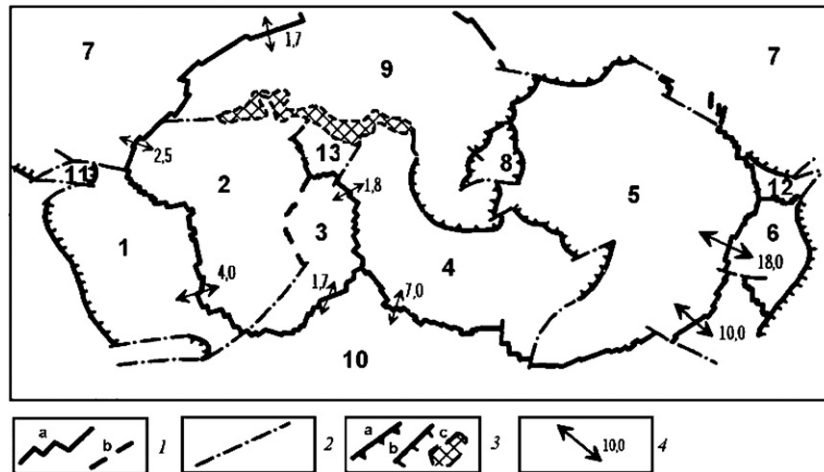


Figure 1. Boundaries of tectonic plates: (1) divergent boundaries (a—oceanic ridges; b—continental rifts), (2) transforming boundaries, (3) convergent boundaries (a—insular; b—active continental outskirts; c—collisions of plates). Directions and velocities of movement of plates (cm year^{-1}).

In addition to the 14 large plates described above there are 38 smaller plates (Okhotsk, Amur, Yangtze, Okinawa, Sunda, Burma, Molucca Sea, Banda Sea, Timor, Birds Head, Maoke, Caroline, Mariana, North Bismarck, Manus, South Bismarck, Solomon Sea, Woodlark, New Hebrides, Conway Reef, Balmoral Reef, Futuna, Niufo’ou, Tonga, Kermadec, Rivera, Galapagos, Easter, Juan Fernandez, Panama, North Andes, Altiplano, Shetland, Scotia, Sandwich, Aegean Sea, Anatolia, Somalia), for a total of 52 plates.

It is commonly accepted that the tectonic plates are relatively thin elastic structures, approximately 100 km thick, with linear size from 1000 km to several thousand km. The material of the plates, at the depth 100 km has typical Young’s modulus $17.28 \times 10^{10} \text{ kg m}^{-1} \text{ s}^{-2}$, density 3380 kg m^{-3} and Poisson coefficient 0.28. The velocity of the longitudinal waves in these materials is approximately 8000 m s^{-1} , and the velocity of the flexural eigen-waves depends on the eigenvalues and varies, depending on the type of the wave, on a wide range around 4500 m s^{-1} , see formula (4) below. Because of non-accurate matching of the boundaries of the neighboring plates, the zones of direct contact of the plates are typically small—about 100 km—compared with the linear size of the plates. Remaining inter-plate space is filled with loose materials, which are not able to accumulate any essential amount of elastic energy caused by the deformation. These materials can damp oscillations with short periods as 20 min–1 h. Damping of acoustic waves by loose materials was discussed in [11, 19, 35]. Since tectonic plates are relatively thin, a major part of their kinetic energy is stored in the form of oscillatory flexural modes. The underlying layer of the asthenosphere makes flexural oscillation of plate possible, but also helps damping of the flexural waves with short periods, due to non-zero viscosity. Based on above data we conjecture that the flexural modes in different tectonic plates, in a certain range of periods, supposedly between 0.2 h–1 h, see below the estimation of periods of eigen-modes of a model rectangular plate, are elastically disconnected from each other. Thus we expect that these flexural modes characterize elastic properties of the plates, but not the global elastic properties of the Earth’s crust.

The convective flows in the asthenosphere and variations of the angular speed of Earth, thanks to long-time variations of the moment of inertia of Earth, may cause collisions of neighboring plates. In presence of the liquid friction on the underlying layer of the asthenosphere, variations of the angular speed of earth cause mutual displacements of the neighboring plates, because small plates react immediately on the variations of the angular speed, and larger plates lag behind. These displacements cause collisions of the plates in the active zones, where the plates directly contact each other. Generally, when the angular speed of Earth decreases, with growing of the moment of inertia due to displacement of the center of gravity of Earth, the collisions may occur on the eastern boundaries of the major plates contacting smaller plates, observe, for instance, the contact of the Euro-Asia plate and the Philippines plate on figure 1. The stress caused by the collision may be either discharged due to forming cracks in the plates, splitting the active zone into independently moving fragments, or, being applied for an extended period of time, may cause accumulation of a considerable amount of (potential) elastic energy in the active zones of contacts, in the form of elastic deformation of the stressed plates. This energy may be eventually discharged in the form of a powerful earthquake.

Accumulation of the elastic energy, due to standard variational principle [7], causes the *increment of eigenfrequencies* of the tectonic plates. In [27, 32, 33] oscillatory processes, with similar spectral characteristics, were observed in mutually remote zones of the Euro-Asia plate. The authors of [27] suggested calling the processes *seismo-gravitational oscillations of the Earth* (SGO). Recent analysis, based on data of the international GEOSCOPE network, revealed the existence of *global* oscillations with periods 3.97 h, 3.42 h, 1.03 h and 0.98 h. SGO with smaller periods do not have global character. They are usually observed in certain plates. For measurements of SGO, special devices are used ('vertical pendulum'), with high sensitivity to the variations of amplitudes and frequencies of SGO within the interval of periods 0.2–2 h. Modification of the registering channel of the device allowed us to extend the interval to 0.2–6 h. Results of analysis of measurements of SGO with relatively short periods from this range are presented in [30]. The data on SGO with longer periods and characteristics of modern 3-channel seismographs can be found in [29]. Observations with these devices reveal a wide spectrum of SGO. Some of the measured frequencies of SGO coincide with short-time variations of the angular speed of Earth, which were estimated based on astronomical observations, see [28]. All experimental data confirm the presence of active energy in the system of tectonic plates, relevant to the inhomogeneity of the lithosphere. Direct calculations of eigenfrequencies of the flexural modes of a rectangular thin plate $\Omega = d_1 \times d_2$, $d_1 = 4000$ km, $d_2 = 8000$ km, 200 km thick, were done, see [21], based on the bi-harmonic model, under natural assumptions concerning the density of the material to be 3380 kg m^{-3} , the Young's modulus is $17.28 \times 10^{10} \text{ kg m}^{-1} \text{ s}^{-2}$ and the Poisson coefficient is equal to 0.28. Though the Young's modulus of a tectonic plate varies on a wide range of values, it is possible to provide a rough estimation, see below, of the periods of SGO and the length of the corresponding running waves of a tectonic plate, by computing these parameters for a model rectangular plate with elastic parameters equal to those of the tectonic plate on the half depth, 100 km. Indeed, the corresponding dynamical equation for the transversal (vertical) displacement f is

$$\rho \frac{\partial^2 f}{\partial t^2} + \frac{h^2 E}{12(1 - \sigma^2)} \Delta^2 f = 0. \quad (1)$$

In [21] the simplest Neumann boundary conditions $\frac{\partial u}{\partial n} \Big|_{\partial \Omega} = \frac{\partial \Delta u}{\partial n} \Big|_{\partial \Omega} = 0$ are imposed on the boundary. This allows us to solve the dynamical equation by Fourier method, via separation of variables. The eigenfunctions of the bi-harmonic operator coincide with the eigenfunction

of the Neumann Laplacian, $f_{l_1, l_2} = \cos \frac{\pi l_1 x_1}{d_1} \cos \frac{\pi l_2 x_2}{d_2}$, but the eigenvalues of the Neumann bi-harmonic operator

$$\lambda_{l_1, l_2}^{\Delta^2} = [\lambda_{l_1, l_2}^{\Delta}]^2 = [\pi^2 (l_1^2 d_1^{-2} + l_2^2 d_2^{-2})]^2$$

are squares of the corresponding eigenvalues of the Neumann Laplacian. Taking into account that

$$\frac{h^2 E}{12\rho(1 - \sigma^2)} = 0.16710^{20} = [0.64 \times 10^5]^4 =: \alpha^4,$$

we find the periods of flexural eigen-oscillations from the formula

$$\omega_{l_1, l_2}^2 = \left(\frac{2\pi}{T_{l_1, l_2}} \right)^2 = \alpha^4 [\lambda_{l_1, l_2}^{\Delta}]^2,$$

or

$$\omega_{l_1, l_2} = \frac{2\pi}{T_{l_1, l_2}} = \alpha^2 \lambda_{l_1, l_2}^{\Delta} =: \alpha^2 k_{l_1, l_2}^2, \tag{2}$$

where k plays the role of the corresponding momentum. The speed of the flexural waves is calculated as

$$v_{l_1, l_2}^f = \frac{\partial \Omega}{\partial k} = 2\alpha k_{l_1, l_2}. \tag{3}$$

Then for the above model plate the periods of flexural oscillations are defined by the formula $T_h = 2.63[4l_1^2 + l_2^2]^{-1}$ h, and the velocity of the corresponding flexural waves are calculated as $v_{l_1, l_2}^f = 3400\sqrt{4l_1^2 + l_2^2}$ m s⁻¹. In particular, the period of the flexural oscillation $f_{1,2}$ and the speed of the corresponding flexural wave $v_{1,2}^f$ are calculated as

$$T_{1,2} = 0.33 \text{ h}, \quad v_{1,2}^f = 9520 \text{ m s}^{-1}, \tag{4}$$

and less for longer periods. The corresponding space-temporal oscillatory mode is

$$\cos \omega_{1,2} t \cos \frac{\pi x_1}{4000} \cos \frac{\pi 2x_2}{8000},$$

with x_1, x_2 measured in kilometers. This oscillatory mode can be represented as a linear combination of running flexural waves

$$\cos \left[\omega_{12} t \pm \frac{\pi x_1}{4000} \pm \frac{\pi x_2}{4000} \right]. \tag{5}$$

The corresponding wavelength is estimated by the minimum of $\sqrt{\Lambda_1^2 + \Lambda_2^2}$, where Λ_1, Λ_2 correspond to the shift of the running wave by the corresponding period in time. For instance

$$\omega_{1,2} T_{12} = 2\pi = \frac{\pi \Lambda_1 + \pi \Lambda_2}{4000}$$

gives an estimation of the minimal wavelength as $\sqrt{\Lambda_1^2 + \Lambda_2^2} \geq 5656$ km, which is much more than the diameter of the active zone, $5656 \text{ km} \gg 100 \text{ km}$. Hence the zero-range model can be used, under above assumption, for the model stressed plate.

It appeared that periods of the eigen-modes $f_{1,1}-f_{5,5}$ sit in the interval 0.21–5 h and their total number and distribution looks similar, see figure 2, to SGO described in the paper [27, 32, 33], despite the trivial plane rectangular geometry of the plate and trivial Neumann boundary conditions.

Examination of the results observed in [27, 32, 33] and theoretically obtained in [21] resulted in the conjecture that flexural SGO *can be interpreted as flexural eigen-modes* of the

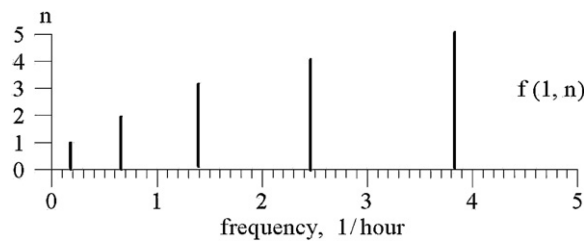


Figure 2. Computed eigenfrequencies of the rectangular plate 4000 km × 8000 km for the modes $f(1, N)$

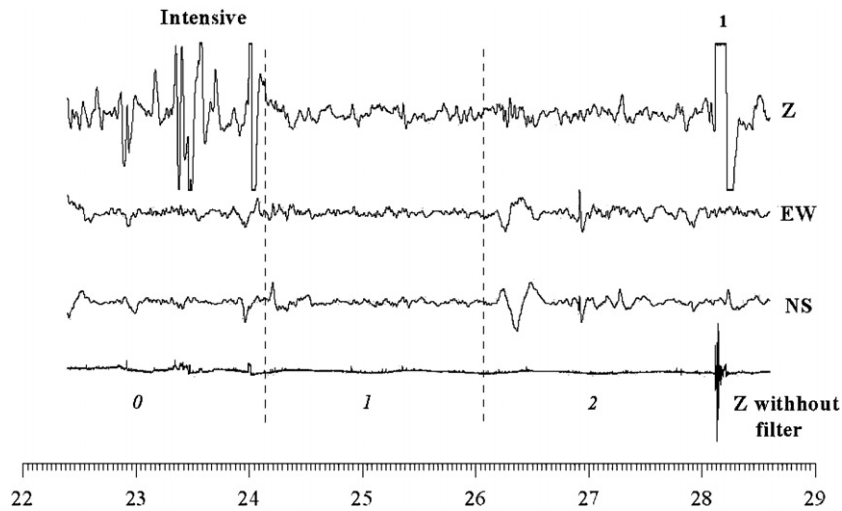


Figure 3. Dynamics of seismo-gravitational oscillations observed in St Petersburg, 22–29 March 2000, see the text below.

relatively thin tectonic plates. We hope that the zero-range model may be also used in this periods range for real tectonic plates as well.

In the following section we model dynamics of tectonic plates based on the bi-harmonic boundary problem with ‘natural’ boundary conditions.

Variation of the character of SGO is seen from comparison of the graphs of the amplitudes of SGO on 48 h intervals of time separated by the vertical dotted lines. The graphs on these intervals show the reaction of the device on the oscillations of the ground.

A typical phenomenon of intense seismo-gravitational *pulsation* (SGP) was registered on the vertical component Z on the initial interval marked by 0. This phenomenon was also noted in the earlier paper [13]. See more about SGP in the further text, after figure 4.

The components Z, EW and NS are obtained after filtration. The graph on the interval 1 shows the reaction of the filter on the maximal phase of the earthquake 28 March 2000 in Japan. The non-filtered graph Z represents the reaction of the base of the vertical seismograph on the flexural oscillations of the ground.

Spectral-time cards, see below figure 4 represents the effect of growing of frequencies of SGO in visual form. The data of the observations were filtered by the band filter with the band strip (60–300 min). We used the gliding time window length 700 min, and step-wise shifts

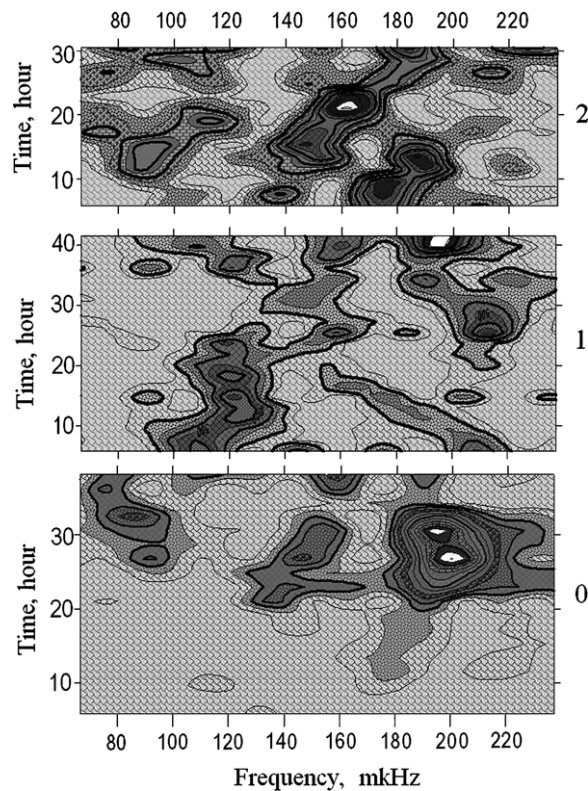


Figure 4. Time–frequency analysis of the vertical component of SGO.

with the 5 min steps. The interval of frequencies, measured in micro-Hertz, was chosen as $[70 \text{ mcHz}, 250 \text{ mcHz}] =: [F_{\min}, F_{\max}]$. For resolution 0.034 mcHz the steps were halved to guarantee better smoothness of the spectral function.

Effect of growing of the frequency of SGO was detected only on spectral-time cards (ST-cards) of the vertical component of SGO, see below figure 4. The frequencies are marked on the horizontal axes, time in hours—on the vertical axes, for the intervals 0,1,2, respectively. The level of spectral amplitudes is represented by the variation of the color. Oscillations with large spectral amplitudes, higher than the average level on the spectrum, are marked by gray color. The maximal amplitudes are marked by white color. The values of these amplitudes on the interval 0 are 3.5 times greater than the average amplitude, (frequency about 200 mcHz). On the interval 1 they exceed the average amplitude in 1.8 times (the frequency about 200 mcHz). On the interval 2 they exceed the average amplitude in 3 times (the frequency about 160 mcHz). For SGO with frequencies 90–110 mcHz and 170–190 mcHz the amplitudes are 1.75 and 2.75 times larger than the average amplitude. All three parts 0,1,2 of figure 4 reveal two patterns of inclined gray domains (left-down to right-up and left-up to right-down) which correspond to SGO with growing and decreasing frequencies, correspondingly. This patterns provide an evidence of increment of the stored elastic energy in the system and discharging the stored elastic energy, respectively in form of oscillation modes with certain frequencies.

Growing of the frequency on the interval 2:

- (1) The frequency is growing from $f_{\min} = 80 \text{ mcHz}$ to 123 mcHz during the period of 15 h.

- (2) The frequency is growing from $f_{\min} = 130$ mcHz to 185 mcHz during the period of 28.5 h.
- (3) The frequency is growing from $f_{\min} = 170$ mcHz to 200 mcHz during the period of 8 h.

Growing of the frequency on the interval 0:

- (1) The frequency is growing from $f_{\min} = 165$ mcHz to 205 mcHz during the period of 33 h.
- (2) The frequency is growing from $f_{\min} = 125$ mcHz to 165 mcHz during the period of 15 h.

Growing and decreasing of frequencies of SGO are easily noticeable also on the interval 1.

Growing of the frequency is characterized by the ratio $\frac{\Delta\nu}{\tau}$, where $\Delta\nu$ is the increment of the frequency and τ is the corresponding time interval, when the growing was observed.

Other domains, where the frequency of the modes decrease with time growing, may be interpreted as an evidence of local relaxation of the stress, probably caused by local destruction of the plate (forming cracks).

We conjecture that the extended growth of frequencies of the SGO may be considered as a precursor of strong earthquakes. Our ability to extract useful information from the observations of frequencies and the shape of SGO is limited by our understanding of the mechanism of the variation of the frequency and the shape of SGO modes arising from the boundary stress on the tectonic plates.

There were also other observations of the shift of frequencies of selected modes of SGO. Note, that in numerous observations on SGO in Leningrad (St Petersburg) intense short pulses were also recorded. They are constituted by several sinusoidal harmonics with periods from 30 min to 1 h, and the total duration of the process 6–10 h. In several cases they were also followed by powerful earthquakes—in 2–4 days. This process was noted first in [13] and was given the name of ‘seismo-gravitational pulsations’, SGP. Statistical analysis was done based on the data of the 6 months monitoring of SGO in St Petersburg. This analysis confirmed that the connection between SGP and the subsequent strong earthquake is not random, with probability 95%.

Essential information on SGO is obtained from the observation of variations of the frequencies and the shape of the corresponding modes in the remote zone. The typical size of the zone of contact is negligible, pointwise, when compared with the wavelength, which generally can be estimated as $[\lambda^\Delta]^{-1/2}$, see (5).

Although the boundaries of real tectonic plate are not smooth, however details of the local geometry of the boundaries may be neglected compared with the wavelength of typical waves on the plates. Then for SGO with periods 20 min–1 h we may base the theoretical analysis of SGO on the bi-harmonic model for the relatively thin plate with natural boundary conditions. In this paper we also neglect presence of the liquid layer of the asthenosphere underlying the plate, thus reducing the problem to construction of self-adjoint extensions of the 2D bi-harmonic operator.

In [31] we use the fact that characteristics of the seismo-gravitational oscillations in remote zone depend on a *small number of basic parameters*. On one hand, this fact can be interpreted in a spirit of the Saint-Venant principle⁴. On the other hand we were able to interpret this fact in the spirit of operator extensions. Based on this observation we developed in [31] a preliminary version of the above arguments and suggested to use a solvable zero-range model of the tectonic plates under a pointwise boundary stress, caused by the collision of plates. The role of the parameter of the model was played by some 3×3 real Hermitian matrix M , see also the following section. Thus the number of the *Saint-Venant parameters*

⁴ We are grateful to Dr Colin Fox for inspiring discussion concerning the Saint-Venant principle.

for the boundary stressed relatively thin tectonic plate is 6. We presume, that the matrix M defines the type of the stress, depending on mutual positions of the contacting plates at the active zone. There is a good reason to call M the Saint-Venant matrix and the number of the Saint-Venant parameters (6)—the Saint-Venant number. We assume that mutual positions of the plates in active zone, and hence the matrix M remains essentially unchanged during extended period. Thus the matrix M characterizes the type of contact of tectonic plates in this location and remains the same for all earthquakes arising from the given active zone. In this paper, based on the *compensation of singularities* in the fundamental Krein formula, we suggest an explicit formula for the perturbed eigenfunctions of the plate. Comparison of the calculated eigenfunction with the data of the instrumental observations in remote zone, permits, in principle, to *fit* the model, that is, to find the basic matrix M . Once *fitted*, the constructed model would allow us to calculate in explicit form the increment of the eigenvalues and the variations of the shape of the eigenfunctions of the stressed (perturbed) plate depending on the type and the magnitude of the local stress. We assume that the shifts of the eigenfrequencies and the changes of the shape of the eigen-modes can be measured for each active zone. With numerous active stations in the GEOSCOPE and IRIS networks, fitting of the proposed model can be done, eventually, for all active zones on the boundary of each major tectonic plate.

Generically earthquakes hit only one active zone at a time. Then comparing the observed shift of the eigenfrequencies and the variations of the shape of the mode in the remote zone, where the Saint-Venant principle is applicable, with the results of computing based on the model, we will be able to localize the excited active zone based on the observed changes of the eigenfrequencies and the shapes (amplitude, polarization) of the flexural eigen-modes.

Mathematically the zero-range model of the isolated pointwise stressed tectonic plate and a similar zero-range model of the pointwise stressed tectonic plate submerged into environment formed by other plates, intermediate layers and asthenosphere, differ by the type of basic equations, but have a lot in common. In particular, the number of free parameters (6) for the pointwise active zone, in the bi-harmonic model and Lamé model is the same. We interpreted these parameters in the spirit of the Saint-Venant principle as essential parameters describing the shape of the wave process in the remote zone, see [31]. In this paper we obtain the first order approximation for the perturbed eigenfrequencies and eigenfunctions based on a *modified* Krein formula, see [1, 18], for the pointwise stressed thin plate described by the bi-harmonic equation. The explicit representation of the perturbed eigen-modes permits to *fit* the zero-range model suggested in [31] based on results of instrumental measurements of SGO. We also conjecture that the properly fitted solvable model of the stressed tectonic plate may help to enlighten the nature of the pulsations.

2. Zero-range model of the pointwise boundary stress

We may base our approach on the standard mathematical model of the tectonic plate in the form of a thin elastic plate, thickness h , with free edge, or on the 3D Lamé equations for displacements. We consider both options, describing in the following two subsections specific details of both models. Then we develop the common part of the theory, for both models simultaneously.

2.1. Thin plate model for the isolated tectonic plate under the localized boundary stress

Denoting by D the ‘the bending stiffness’, connected with Young modulus E , the thickness h of the plate and the Poisson coefficient σ by the formula $D = Eh^2[12(1 - \sigma^2)]^{-1}$, we

represent, following [12], the corresponding dynamical equation for the normal displacement u as

$$\rho \frac{\partial^2 u}{\partial s^2} = D \Delta^2 u.$$

We consider time-periodic solutions $u(\omega s, x)$ of the equation and separate the time, thereby reducing the dynamical problem to the spectral problem with the spectral parameter

$$\lambda = \rho D^{-1} \omega^2 \tag{6}$$

for a bi-harmonic operator on a compact 2D domain Ω —the tectonic plate—with a smooth boundary $\partial\Omega$

$$Au = \Delta^2 u = \lambda u, \quad u \in W_2^4(\Omega),$$

and free boundary condition involving the tangential and normal derivatives of the displacement u and the tension Δu

$$\left[\frac{\partial \Delta u}{\partial n} + (1 - \sigma) \frac{\partial^3 u}{\partial n \partial t^2} \right] \Big|_{\partial\Omega} = 0, \quad \left[\Delta u - (1 - \sigma) \frac{\partial^2 u}{\partial t^2} \right] \Big|_{\partial\Omega} = 0, \tag{7}$$

where n, t are the normal and the tangent directions on the boundary.

The bi-harmonic operator A is self-adjoint in the Hilbert space $L_2(\Omega) := \mathcal{H}$. The eigenfunctions of A are smooth and they form an orthogonal basis in $L_2(\Omega) = \mathcal{H}$. We consider the restriction A_0 of A onto $D(A_0)$ constituted by all smooth functions vanishing near the boundary point $a \in \partial\Omega$. The restriction is symmetric, but it is not self-adjoint, because the range of it $(A - \lambda I) D(A_0)$, for complex λ has a nontrivial complement N_λ which is a linear hull of the Green function $G(x, a, \bar{\lambda}) := g_0(x, \bar{\lambda})$ and its tangential derivatives $\frac{\partial G(x, a, \bar{\lambda})}{\partial t} := g_1(x, \bar{\lambda})$, $\frac{\partial^2 G(x, a, \bar{\lambda})}{\partial t^2} := g_2(x, \bar{\lambda})$ of the first and second order, at the point a . The orthogonal complement N_λ of the range is called the ‘deficiency subspace’, and elements of it—‘deficiency elements’:

$$N_\lambda := \mathcal{H} \ominus (A_0 - \lambda I) D_0 = \bigvee_{s=0}^2 g_s(*, \bar{\lambda}).$$

The deficiency elements have, at the boundary point a , singularities of different types (see for instance [14], where much more general problem is considered)

$$g_0(n, t) \approx (n^2 + t^2) \ln(n^2 + t^2), \quad g_1(n, t) \approx t \ln(n^2 + t^2), \quad g_2(n, t) \approx \ln(n^2 + t^2),$$

hence they are linearly independent and form a basis in the deficiency subspace. The deficiency subspace at the spectral point $\bar{\lambda}$ is

$$N_{\bar{\lambda}} := \mathcal{H} \ominus (A_0 - \bar{\lambda} I) D_0 = \bigvee_{s=0}^2 g_s(*, \lambda).$$

The dimensions of the deficiency subspaces (3, 3) constitute the ‘deficiency index’. Hereafter we select $\lambda = i$ and attempt to construct a self-adjoint extension of A_0 , which will play a role of a zero-range model of the tectonic plate under the boundary strain.

Note that in the Lamé model the deficiency index is also (3, 3), on a smooth boundary. The role of deficiency elements is played by the columns of the Green matrix. The boundary of the tectonic plates may be assumed smooth for the long waves (small λ), since the integral shape of the solutions of the differential equations with small λ is not affected by the details of the local geometry.

2.2. Construction of the self-adjoint extension

Extend A_0 from D_0 onto $D(A_0^+) = D_0 + N_i + N_{-i}$ as an ‘adjoint operator’ A_0^+ by setting $(A_0^+ \pm iI)g = 0$ for $g \in N_{\mp i}$. This operator not self-adjoint, and it is not even symmetric, so that the boundary form

$$\langle A_0^+ u, v \rangle - \langle u, A_0^+ v \rangle = \mathcal{J}(u, v) \tag{8}$$

does not vanish, generally, for $u, v \in D(A_0^+)$. One can rewrite (8) in more convenient form with using new symplectic coordinates with respect of a new basis in N

$$W_s^+ = \frac{1}{2} \left[g_s + \frac{A+iI}{A-iI} g_s \right] = \frac{A}{A-iI} g_s$$

$$W_s^- = \frac{1}{2i} \left[s_s - \frac{A+iI}{A-iI} g_s \right] = -\frac{I}{A-iI} g_s.$$

Since $A_0^+ g_s + i g_s = 0$, $[A_0^+ - iI] \frac{A+iI}{A-iI} g_s = 0$ we have,

$$A_0^+ W_s^+ = W_s^-, \quad A_0^+ W_s^- = -W_s^+. \tag{9}$$

Following [24] we will use the representation of elements from the domain of the adjoint operator, by the expansion on the new basis

$$u = u_0 + \sum_s \xi_+^s W_s^+ + \xi_-^s W_s^- = u_0 + \frac{A}{A-iI} \sum_s \xi_+^s g_s - \frac{I}{A-iI} \sum_s \xi_-^s g_s$$

$$:= u_0 + \frac{A}{A-iI} \vec{\xi}_+ - \frac{I}{A-iI} \vec{\xi}_-. \tag{10}$$

Note that due to (9)

$$A^+ \frac{A}{A-iI} \vec{\xi}_+ = -\frac{I}{A-iI} \vec{\xi}_+, \quad A^+ \frac{-I}{A-iI} \vec{\xi}_- = -\frac{A}{A-iI} \vec{\xi}_-.$$

Note that the boundary form

$$\langle A_0^+ u, v \rangle - \langle u, A_0^+ v \rangle := \mathcal{J}(u, v)$$

of elements u, v ,

$$u = u_0 + \frac{A}{A-iI} \vec{\xi}_+^u - \frac{I}{A-iI} \vec{\xi}_-^u := u_0 + n^u, \quad u_0 \in D(A_0) n^u \in N,$$

$$v = v_0 + \frac{A}{A-iI} \vec{\xi}_+^v - \frac{I}{A-iI} \vec{\xi}_-^v := v_0 + n^v, \quad v_0 \in D(A_0) n^v \in N \tag{11}$$

depends only on components n^u, n^v of u, v in the defect N . Then the boundary form is represented as

$$\langle A_0^+ u, v \rangle - \langle u, A_0^+ v \rangle := \mathcal{J}(u, v) = \langle \vec{\xi}_+^u, \vec{\xi}_-^v \rangle - \langle \vec{\xi}_-^u, \vec{\xi}_+^v \rangle \tag{12}$$

with Euclidean dot product for vectors $\vec{\xi}_\pm \in N_i$. Note that the representation of the boundary form in terms of abstract boundary values $\vec{\xi}_\pm$ contains only integral characteristics of the elements from the domain of the operators considered, and hence it is stable with respect of minor local perturbations of geometry of the plates. This enables us to substitute, for practical calculations, the real irregular boundaries of the plates by the smoothed boundaries, obtained via elimination of minor geometrical details, compared with the length of standing waves, circa 5000 km, of SGO with periods in the essential range 20 min–1 h.

The boundary form vanishes on the Lagrangian plane defined in $D(A_0^+)$ defined by the ‘boundary condition’ with an Hermitian operator $M : N_i \rightarrow N_i$:

$$\vec{\xi}_+ = M \vec{\xi}_-. \tag{13}$$

This boundary condition defines a self-adjoint operator A_M as a restriction of A_0^\dagger onto the Lagrangian plane $\mathcal{T}_M \in D(A_0^\dagger)$ defined by the boundary condition (13). The resolvent of A_M defined by the boundary conditions is represented, at regular points of A_M , by the Krein formula, see [2, 24]

$$(A_M - \lambda I)^{-1} = \frac{I}{A - \lambda I} - \frac{A + iI}{A - \lambda I} P M \frac{I}{I + P \frac{I + \lambda A}{A - \lambda I} P M} P \frac{A - iI}{A - \lambda I}, \quad (14)$$

where P is an orthogonal projection onto N_i .

2.3. Compensation of singularities in Krein formula and calculation of the perturbed spectral data

Singularities of the resolvent $(A_M - \lambda I)^{-1}$ coincide with the spectrum of A_M . But both terms in the right side of (14) also have singularities on the spectrum of the non-perturbed operator A . *The singularities of the first and second term eigenvalues of A compensate each other.* We are able to derive this statement via straightforward calculation, in classical Krein–Birman–Schwinger formula and in the corresponding construction for quantum networks, see [1, 18]. In the course of the calculation of the compensation of singularities we can recover both the eigenvalues of the perturbed operator A_M and the corresponding eigenfunctions, see [18]. Note that a similar statement, as a lemma on compensation of singularities of the corresponding Weyl–Titchmarsh function, was discovered in [6] for 1D solvable model of the quantum network in the form of a quantum graph. Later, in [16] and in [15], similar statements were proven for Dirichlet-to-Neumann maps of quantum networks. We formulate here this statement for the resolvent of the self-adjoint extension based on ideas proposed in [17].

We will observe the effect of compensation of singularities on a certain spectral interval $\Delta_0 = [\lambda_0 - \delta, \lambda_0 + \delta]$, centered at the *resonance eigenvalue* λ_0 of the non-perturbed plate, assuming that the perturbation defined by the matrix M is relatively small, in a certain sense, see below.

Assuming that there is a single eigenvalue λ_0 of A on the interval Δ_0 , with the eigenfunction φ_0 , we use the following representations, separating the polar terms from smooth operator functions K_i, K_{-1}, K on Δ_0

$$\begin{aligned} \frac{A + iI}{A - \lambda I} &= (\lambda_0 + i) \frac{\varphi_0 \langle \varphi_0}{\lambda_0 - \lambda} + K_{-i}, \\ \frac{A - iI}{A - \lambda I} &= (\lambda_0 - i) \frac{\varphi_0 \langle \varphi_0}{\lambda_0 - \lambda} + K_i, \\ P \frac{I + \lambda A}{A - \lambda I} P &= (1 + \lambda_0^2) \frac{P \varphi_0 \langle P \varphi_0}{\lambda_0 - \lambda} + K(\lambda), \end{aligned} \quad (15)$$

with a smooth matrix function $K = K_0 + o(|\lambda - \lambda_0|)$, with $K_0 = K(\lambda_0)$ and $\|o(|\lambda - \lambda_0|)\| \leq C_0 \delta$.

Definition 2.1. *We say that the matrix M is relatively small, if $[I + K(\lambda)M]^{-1}$ exists and is bounded on Δ_0 .*

This condition is obviously fulfilled if

$$\|[I + K(\lambda_0)M]^{-1}\| C_0 \delta \ll 1. \quad (16)$$

To calculate the second term in the right side of the Krein formula (14) we have to compute the inverse of the denominator, that is to solve the equation

$$\left[I + P \frac{I + \lambda A}{A - \lambda I} M \right] u = g. \quad (17)$$

Though the standard analytic perturbation technique is still not applicable to this equation under the above conditions 2.1 or (16), we are able to construct the inverse based on finite dimensionality (one-dimensionality) of the polar term.

$$u = [I + KM]^{-1}g - (1 + \lambda_0^2) \frac{[I + KM]^{-1}P\varphi_0 \langle P\varphi_0 M[I + KM]^{-1}g \rangle}{\lambda_0 - \lambda + \langle P\varphi_0 M[I + KM]^{-1}\varphi_0 \rangle}. \quad (18)$$

Based on (18) we are able, see [1, 18] to observe the compensation of singularities in the above Krein formula (14) and calculate the polar term of the resolvent at the single eigenvalue of the operator A_M on the interval Δ_0 .

Theorem 2.1. *If the perturbation is relatively small, as required in (2.1), then there exists a single eigenvalue λ_M of the perturbed operator A_M on the interval Δ_0 which is found as a zero of the denominator in (18)*

$$\lambda_0 - \lambda + (1 + \lambda_0^2) \langle P\varphi_0 M[I + KM]^{-1}\varphi_0 \rangle := \mathbf{d}_M(\lambda), \quad \mathbf{d}_M(\lambda_M) = 0 \quad (19)$$

and the corresponding eigenfunction

$$\varphi_M = \varphi_0 - (\lambda_0 - i)K_{-i}M[I + KM]^{-1}P\varphi_0, \quad (20)$$

computed at the zero λ_M . The polar term of the resolvent of the perturbed operator at the eigenvalue is represented as

$$\frac{\varphi_0 - (\lambda_0 - i)K_{-i}M[I + KM]^{-1}P\varphi_0 \langle \varphi_0 - (\lambda_0 - i)K_{-i}M[I + KM]^{-1}P\varphi_0 \rangle}{\mathbf{d}_M(\lambda)}$$

Proof. of this statement can be obtained similarly to the corresponding statement in [18], where the case of several eigenvalues of the non-perturbed operator on an essential spectral interval was discussed. We consider here the simplest case, when only one eigenvalue of the unperturbed plate is present on an essential spectral interval. If the perturbation is small as required by condition (16), then the approximate eigenvalue and the corresponding approximate eigenfunction of A_M can be obtained via replacement of $K, K_{\pm i}$ into (19), (20) by $K(\lambda_0), K_{\pm i}(\lambda_0)$

$$\begin{aligned} \lambda_M &\approx \lambda_0 + (1 + \lambda_0^2) \langle P\varphi_0 M[I + K(\lambda_0)M]^{-1}K(\lambda_0)\varphi_0 \rangle, \\ \varphi_M &\approx \varphi_0 - (\lambda_0 - i)K_{-i}(\lambda_0)M[I + K(\lambda_0)M]^{-1}P\varphi_0. \end{aligned} \quad (21) \quad \square$$

Remark. Analysis of the multi-point boundary condition which corresponds to several stresses applied at the points a_1, a_2, \dots, a_m on the boundary of the plate Ω differs from the above analysis of the single-point case, only in the first step. In the case of a multi-point stress we have to construct of elements $\{g_0^r(x, a_r, i), g_1^r(x, a_r, i), g_2^r(x, a_r, i)\}_{r=1}^m$ a basis in the larger deficiency subspace $N_i, \dim N_i = 3m$. Due to the presence of singularities of different types at different points, the deficiency elements are linearly independent.

3. Concluding remarks on the fitting of the model

The pair of data (21) may be used in two different ways: either for calculation of the shift of the frequency of SGO and the corresponding perturbation of the eigenfunction, under the pointwise stress characterized by the matrix M , or, vice versa, for recovering of the data on the localization, the type and the intensity of the stress from instrumental observations.

Indeed, if the geological structure of the tectonic plates at the active zones, encoded in matrices M_s attached to the zones, are known, then, theoretically, we are able to calculate the eigenfunctions and the eigenfrequencies of the plates, taking into account the stress caused

by collisions. We are also able, theoretically, to construct the deficiency elements for all active zones. Then the self-adjoint extension of the bi-harmonic operator on the plate, with the pointwise boundary stress, can be constructed, with the corresponding matrices M_s . The obtained theoretical results can be compared with the results of the instrumental measurements. This permits to recover the matrices M_s , which characterize the stressed points a_1, a_2, \dots .

Assume that the structure of the plates at the collision point a remains unchanged, but the tension is growing linearly with time τ as $M(\tau) = m\tau$, with a matrix coefficient $m : N \rightarrow N$. Then the formulae (20), (19), for small τ , define the derivatives of λ_M, φ_M with respect to τ at the moment $\tau = 0$

$$\left. \frac{\partial \varphi_M}{\partial \tau} \right|_{\tau=0} = -(\lambda_0 - i)K_{-i}m_0P_+\varphi_0(x_s), \quad \left. \frac{\partial \lambda_M}{\partial \tau} \right|_{\tau=0} = (1 + \lambda_0^2)\langle P_+\varphi_0, mP_+\varphi_0 \rangle.$$

Comparing this result with ratios

$$\left. \frac{\varphi_{m\tau}(x_s) - \varphi_0}{\tau} \right|_{\tau=0}(x_s), \quad \left. \frac{\lambda_{m\tau} - \lambda_0}{\tau} \right|_{\tau=0},$$

measured experimentally for the amplitude and frequency of SGO, we are able to find fit m , and calculate the increment of $M\delta M = \tau m$.

Practical experience in analytic perturbations shows, that minor perturbations affect rather the eigenvalues, than the shapes of the eigenfunctions of the spectral problem. Based on this observation we can estimate the speed of accumulation of elastic energy \mathcal{E} , under the pointwise boundary stress depending on the speed of the shift of the eigenvalues (eigenfrequencies) of SGO and initial distribution of the elastic energy on the modes φ_0^s defined by the corresponding Fourier coefficients $\langle u, \varphi_0^s \rangle$

$$\frac{d\mathcal{E}}{d\tau} \approx \sum_s \frac{d\lambda_M^s}{d\tau} |\langle u, \varphi_0^s \rangle|^2 = \sum_s (1 + (\lambda_0^s)^2) \langle P_+\varphi_0^s, mP_+\varphi_0^s \rangle |\langle u, \varphi_0^s \rangle|^2,$$

with the summation extended only on the eigen-modes which correspond to the varying eigenvalues. If only one active zone a_s is involved at a time, then only one matrix M_s has to be taken into account, so that the risk of the powerful earthquake may be estimated based on the magnitude of $\delta_s = \tau m_s$.

If there are several active zones at the points a_1, a_2, \dots, a_n on the boundary of the plate, then the corresponding matrices M_1, M_2, \dots, M_n can be fitted based on observations of SGO in the remote zone during preceding earthquakes which occurred at a_1, a_2, \dots, a_n . Variations of the frequencies and the shape of SGO may arise from the stress at any active zone, but usually only one active zone is involved at a time. Once the matrices M_1, M_2, \dots , are known, then comparison of the perturbation of the frequencies and the shapes of seismo-gravitational modes, SGM (or, probably, seismo-gravitational pulsations, SGP) at the given groups of points in the remote zone with results of previous measurements at these points, would allow us to identify the active zone where the stress is applied. We presume that the above model gives a chance to introduce a useful system into the scope of the experimental data on the seismo-gravitational oscillations in remote zone and use them for estimating of risk and localization of the powerful earthquakes. This opens an alternative to the statistical methods, see [34], of estimation of risk of powerful earthquakes.

Fitting of the proposed model in reality requires both extended computing and a major experimental data base. Because the wavelengths of the standing waves, circa 5000 km, on the essential range of periods, 20 min–1 h, dominate the size of the active zones, one may assume, that the straightforward computing with averaged and smoothed data for Young’s modulus and geometric characteristics of the plates will enable us to obtain a realistic approximation of

the deficiency elements, with singularities at the active zones, and to construct the perturbed eigenfunctions of the plates, which correspond to SGO.

More accurate theory requires taking into account realistic boundary conditions, and the exchange of energy with the liquid underlay and neighboring plates. In particular, arising new modes in the spectrum of SGO of the plate, transferred, due to the tight contact in active zone, from the neighboring plate may be considered as another possible precursor of a powerful earthquake. The choice of realistic boundary conditions has to be done based on experimental data interpreted within an appropriate extension of the scheme proposed above, with Lamé and hydro-dynamical equations involved. We postpone discussion of these interesting questions to oncoming publications.

Acknowledgments

The initial version of the text was presented at the IG Petrovskii conference Moscow, May 21–26, 2007, see [26], and issued as a preprint of the Semester of Quantum Graphs at the International Newton institute, Cambridge, January–June 2007, see [22]. The authors acknowledge support from the organizers and participants of these meetings. The authors are grateful to Doctor Colin Fox for an inspiring discussion of the Saint-Venant principle. L Petrova acknowledges support from the RFFI grant 01-05-64753, B Pavlov acknowledges support from the grant of the Russian Academy of Sciences, RFFI 97-01-01149.

References

- [1] Adamyan V, Pavlov B and Yafyasov A 2007 Modified Krein formula and analytic perturbation procedure for scattering on arbitrary junction *Preprint of the International Newton Institute, NI07016* 30 p
- [2] Akhiezer N I and Glazman I M 1966 *Theory of Linear Operators in Hilbert Space* vol 1 (New York: Frederick Ungar, Publ.) (translated from Russian by M Nestel)
- [3] Aplonov S V 2001 *Geodinamika* (Sankt-Petersburg: Sankt-Petersburg University) 360 p (in Russian)
- [4] Albeverio S and Kurasov P 2000 *Singular Perturbations of Differential Operators. Solvable Schrödinger Type Operators* (London Mathematical Society Lecture Note Series vol 271) (Cambridge: Cambridge University Press) xiv+429 pp
- [5] Berezin F A and Faddeev L D 1961 A remark on Schrödinger equation with a singular potential *Sov. Math. Dokl.* **2** 372–6
- [6] Bogevolnov V, Mikhailova A, Pavlov B and Yafyasov A 2001 About scattering on the ring *Operator Theory: Advances and Applications* vol 124 (Israel Gohberg Anniversary volume) ed A Dijksma, A M Kaashoek and A C M Ran (Basel: Birkhäuser) pp 155–87
- [7] Courant R and Hilbert D 1968 *Methoden der mathematischen Physik. I. (German) Dritte Auflage, Heidelberger Taschenbücher, Band 30* (Berlin: Springer) xv+469 p
- [8] Demkov Yu N and Ostrovskij V N 1988 *Zero-Range Potentials and their Applications in Atomic Physics* (New York: Plenum)
- [9] Fermi E 1936 Sul motto dei neutroni nelle sostanze idrogenate *Ric. Sci.* **7** 13 (in Italian)
- [10] Karpeshina Yu E and Pavlov B S 1986 Interactions of the zero radius for the bi-harmonic and the poly-harmonic equations *Mat. Zametki* **40** 49–59, 140 (in Russian)
Karpeshina Yu E and Pavlov B S 1987 *Math. Notes* **40** 528–33 (Engl. Transl.)
- [11] Kuperin Y A 1979 On acoustic properties of vibration protection of the reactor PIK *Preprint of Leningrad Institute of Nuclear Physics Gatchina* 23 p (in Russian)
- [12] Landau L D and Lifschitz E M 1991 *Lehrbuch der theoretischen Physik ('Landau-lifschitz') Band VII (German) (Textbook of theoretical physics ('Landau-Lifschitz') vol VII) Elastizitätstheorie (Elasticity Theory)* 7th edn (Berlin: Akademie-Verlag) 223 p (translated from the Russian by B Kozik and W Göhler)
- [13] Lin'kov E M, Petrova L N and Osipov K S 1992 *Seismogravitational Pulsations of the Earth and Atmospheric Perturbations as Possible Precursors to Strong Earthquakes (Doklady the USSR Academy Sciences: Earth Sci. Section)* **306** pp 76–9 (translations)
- [14] Mazja V G and Plamenevskii B A 1977 The coefficients in the asymptotic form of the solution of elliptic boundary value problem in domains with conical points *Math. Nachrichten* **76** 29–60

- [15] Mikhailova A and Pavlov B 2002 Resonance quantum switch, *Operator Methods in Ordinary and Partial Differential Equations: S Kovalevski Symp. (University of Stockholm, June 2000)* vol 132 ed S Albeverio, N Elander, W N Everitt and P Kurasov (Basel: Birkhauser) pp 287–322
- [16] Mikhailova A and Pavlov B 2001 Quantum domain as a triadic relay *Unconventional Models of Computations: UMC'2K (Springer Verlag Series for Discrete Mathematics and Theoretical Computer Science)* ed I Antoniou, C Calude and M J Dinneen pp 167–86
- [17] Mikhailova A, Pavlov B and Prokhorov L 2003 *Modelling of quantum networks* 69 p (Preprint [math-ph/031238](#))
- [18] Mikhailova A and Pavlov B 2006 Remark on compensation of singularities in Krein formula *Operator Theory: Advances and Applications: Proc. OTAMP06 (Lund, June 2006)* ed P Kurasov, A Laptev and S Naboko 9 p, at press
- [19] Nigmatulin R I 1978 *Foundations of the Mechanics of Heterogeneous Media* (Moscow: Nauka) 336 p (in Russian)
- [20] von Neumann J 1996 Mathematical foundations of quantum mechanics *Princeton Landmarks in Mathematics (Princeton Paperbacks)* twelfth printing (Princeton, NJ: Princeton University Press) xii+445 pp (translated from the German and with a preface by Robert T Beyer)
- [21] Osipov K S 1992 Adaptive analysis of the non-stationary time series in study of seismic oscillations with periods 0.5–5 hours *PhD Thesis* Sankt-Petersburg University 110 p (in Russian)
- [22] Pavlov B and Petrova L 2007 The problem of fitting of the zero-range model of the tectonic plate under a localized boundary stress *International Newton Institute Report Series NI 07027* (Cambridge, 30 April) 19 p
- [23] Pavlov B and Kruglov V 2005 Operator extension technique for resonance scattering of neutrons by nuclei *Hadronic J.* **28** 259–68
- [24] Pavlov B 1987 The theory of extensions and explicitly-solvable models *Russ. Math. Surv.* **42** 127–68
- [25] Pavlov B 2007 A star-graph model via operator extension *Mathematical Proc. of the Cambridge Philosophical Society* March vol 142 pp 365–84
- [26] Pavlov B Saint-Venant principle and an explicitly-solvable model of a thin plate under a pointwise boundary stress *Int. Conf.: Differential Equations and Related Topics (dedicated to I G Petrovskii) Book of Abstracts (Moscow, 21–26 May)* p 236
- [27] Petrova L N, Lin'kov E M and Zuroshvili D D 1988 Planetary Character of Superlong Oscillations of Earth (*Vestnik LGU, vyp. 4(25) 4*) pp 21–26 (in Russian)
- [28] Petrova L N and Lybimtsev D V 2006 Global nature of the seismogravitational oscillations of the earth *Izvestiya, Phys. Solid Earth* **42** 114–23
- [29] Petrova L N, Orlov E G and Karpinsky V V 2007 On dynamics and structure of oscillations of Earth in December 2004 according to observations on seismogravimeter in St. Petersburg *Izvestiya, Phys. Solid Earth* **43** 111–8
- [30] Petrova L N 2008 Oscillations of the Earth with periods from 9 min to 57 min in the background seismic process and the energy flux direction in the range of the free oscillation ${}_0S_2$ *Izvestiya, Phys. Solid Earth* **44** 1–14 at press
- [31] Petrova L N, Pavlov B S and Ivlev L S 2008 On the issue of seismographical oscillations of Earth: perturbation of eigenfrequencies of a thin plate under a pointwise boundary strain *Proc. Inter-Regional Conf.: Ekologiya i kosmos 2007* (Saint-Petersburg University) pp 108–18 (in Russian)
- [32] Petrova L N 2000 The seismic process in the frequency range 0.05-0.5 mHz: patterns and peculiarities *Volc. Seis.* **21** 573–85
- [33] Petrova L N 2002 Seismogravitational oscillations of the earth from observations by spaced vertical pendulums in Eurasia *Izvestiya, Phys. the Solid Earth* **38** 325–36
- [34] Smith W 2005 (GNS Science Lower Hutt, New Zealand) Earthquake risk assessment: from scientific research to risk management decisions *Science and Security Conf. RSNZ (Wellington, 17 Nov. 2005)* session 2
- [35] Xiaofan Li 2001 Scattering of seismic waves in arbitrarily heterogeneous and acoustic media: a general solution and simulations *Geophys. Res. Lett.* **28** 3003–6